7. Transonic Aerodynamics of Airfoils and Wings

7.1 Introduction

Transonic flow occurs when there is mixed sub- and supersonic local flow in the same flowfield (typically with freestream Mach numbers from M = 0.6 or 0.7 to 1.2). Usually the supersonic region of the flow is terminated by a shock wave, allowing the flow to slow down to subsonic speeds. This complicates both computations and wind tunnel testing. It also means that there is very little analytic theory available for guidance in designing for transonic flow conditions. Importantly, not only is the outer inviscid portion of the flow governed by nonlinear flow equations, but the nonlinear flow features typically require that viscous effects be included immediately in the flowfield analysis for accurate design and analysis work. Note also that hypersonic vehicles with bow shocks necessarily have a region of subsonic flow behind the shock, so there is an element of transonic flow on those vehicles too.

In the days of propeller airplanes the transonic flow limitations on the propeller mostly kept airplanes from flying fast enough to encounter transonic flow over the rest of the airplane. Here the propeller was moving much faster than the airplane, and adverse transonic aerodynamic problems appeared on the prop first, limiting the speed and thus transonic flow problems over the rest of the aircraft. However, WWII fighters could reach transonic speeds in a dive, and major problems often arose. One notable example was the Lockheed P-38 Lightning. Transonic effects prevented the airplane from readily recovering from dives, and during one flight test, Lockheed test pilot Ralph Virden had a fatal accident. Pitching moment change with Mach number (Mach tuck), and Mach induced changes in control effectiveness were major culprits.[1]

The invention of the jet engine allowed aircraft to fly at much higher speeds (recall that the Germans used the Me 262 at the end of WWII, in 1944, and the Gloster Meteor was apparently the first operational jet fighter). Since the advent of the jet engine, virtually all commercial transports now cruise in the transonic speed range. As the Mach number increases, shock waves appear in the flowfield, getting stronger as the speed increases. The shock waves lead to a rapid increase in drag, both due to the emergence of wave drag, and also because the pressure rise through a shock wave thickens the boundary layer, leading to increased viscous drag. Thus cruise speed is limited by the rapid drag rise. To pick the value of the Mach number associated with the rapid increase in drag, we need to define the *drag divergence Mach number*, M_{DD}. Several definitions are available. The one used here will be the Mach number at which $dC_D/dM = 0.10$.

After WWII, it was found that the Germans were studying swept wings to delay the drag rise Mach number. Allied examination of German research led to both the North American F-86 and the Boeing B-47 designs being changed to swept wing configurations. The idea of swept wings can be traced to Busemann's Volta conference paper of 1935, and the wartime ideas of R.T. Jones at the NACA. Ironically, the airplane used for the first manned supersonic flight (the X-1, in 1947), did not use a jet engine or wing sweep. It was a rocket powered straight wing airplane. However, shortly thereafter, the F-86, a swept wing jet powered fighter, went supersonic in a shallow dive.

Thus, advances in one technology, propulsion, had a major impact on another, aerodynamics, and illustrates the need to carefully integrate the various technologies to achieve the best total system performance. The formal process of performing this integration has become known as multidisciplinary design optimization (MDO).

7.2 Physical aspects of flowfield development with Mach number.

Figure 7-1, taken from the classic training manual, *Aerodynamics for Naval Aviators*,[2] shows the development of the flow with increasing Mach number, starting from subsonic speeds. At some freestream Mach number the local flow becomes sonic at a single point on the upper surface where the flow reaches its highest speed locally. This is the *critical Mach number*. As the freestream Mach number increases further, a region of supersonic flow develops. Normally the flow is brought back to subsonic speed by the occurrence of a shock wave in the flow. Although it is possible to design an airfoil to have a shock-free recompression, this situation is usually possible for only a single combination of Mach number and lift coefficient. As the Mach number increases, the shock moves aft and becomes stronger. As the Mach number continues to increase, a supersonic region and shock wave also develops on the lower surface. As the Mach number approaches one, the shocks move all the way to the trailing edge. Finally, when the Mach number becomes slightly greater than one, a bow wave appears just ahead of the airfoil, and the shocks at the trailing edge become oblique. These shock waves are the basis for the sonic boom. Many variations in the specific details of the flowfield development are possible, depending on the specific geometry of the airfoil.

This typical progression of the flow pattern, as shown in Figure 7-1, leads to rapid variations in drag, lift and pitching moment with change in Mach number. Today we can predict these variations computationally. However, when these changes were initially found in flight, they were dangerous and appeared mysterious to designers because there was no understanding of the fluid mechanics of the phenomena.

Note that problems with pitching moment variation with Mach number and the flowfield over a control surface using a hinged deflection led to the introduction of the all-flying tail in the X-1 and later models of the F-86. Subsequently, all-flying tails became standard on most supersonic tactical aircraft. This was considered an important military advantage, and was classified for several years.

Based on military experience, Lockheed used an all-flying tail on the L-1011, while the other transport manufacturers continued to use a horizontal tail and elevator.

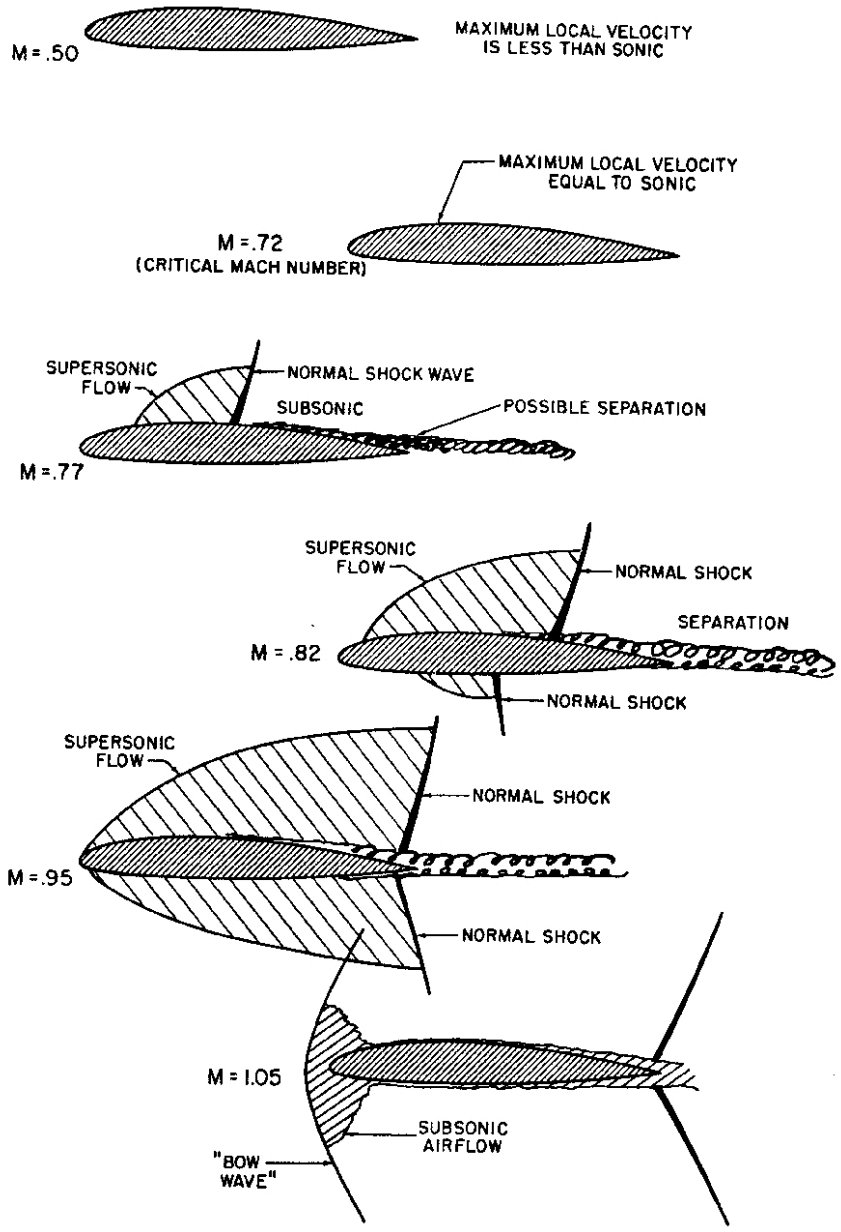

Figure 3.9. Transonic Flow Patterns (sheet 1 of 2)

Figure 7-1. Progression of shock waves with increasing Mach number, as shown in *Aerodynamics for Naval Aviators*,[2] a classic Navy training manual (not copyrighted).

7.3 Technology Issues/developments

7.3.1 The slotted wall wind tunnel

Several advances in technology were key to our ability to design efficient transonic aircraft. The problem with wind tunnel testing was the reflection of shocks from the tunnel walls and the

tendency of the flow to choke as it went past the model. Wind tunnel results were completely wrong. The invention of the slotted wall wind tunnel at NACA Langley in the late 1940s allowed the tunnel interference effects to be significantly reduced, and led to practical wind tunnel testing methods. A chapter in Becker's book describes how this capability came about.[3] The slots are clearly shown in Figure 7-2. Using the 8-foot slotted wall wind tunnel at NASA Langley, Whitcomb, who had earlier developed the area rule, made a breakthrough in airfoil design. His *supercritical airfoil* designs spurred renewed interest in airfoil design for increased efficiency at transonic speeds.[4] His group also had to figure out how to simulate the full scale Reynolds number at sub scale conditions.[5] Finally, in the early 1970s, breakthroughs in computational methods produced the first transonic airfoil analysis codes, which are described briefly in the next section.

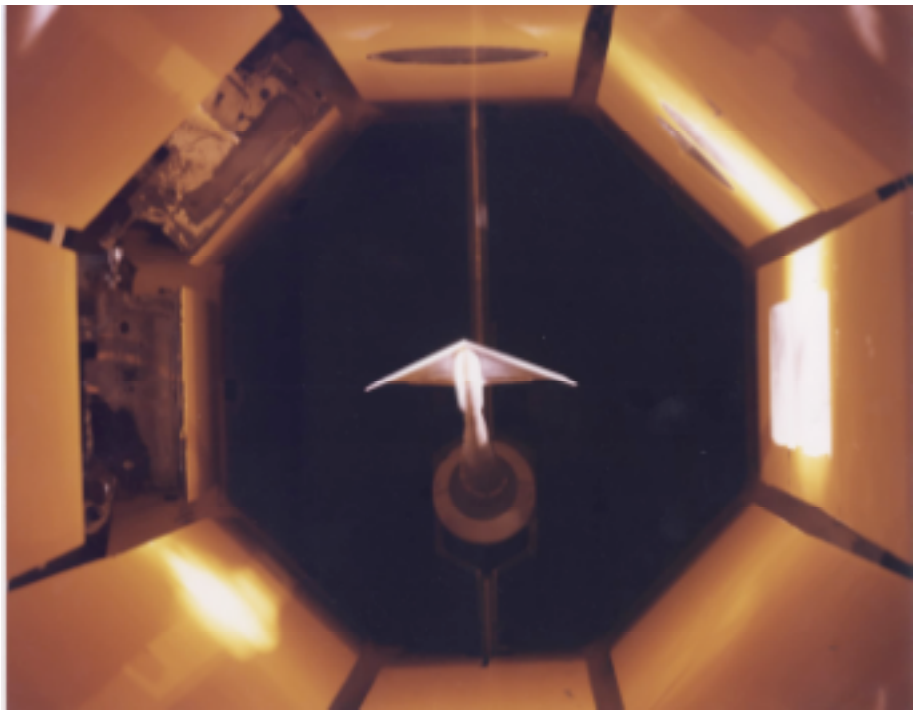

Figure 7-2. A slotted wall wing tunnel test section. This picture is of a small blow-down tunnel design that was used to validate the concept before the large continuous-flow tunnels were constructed at NACA Langley Research Center. This specific tunnel is a copy of the one made at Langley and was constructed by Republic Aviation in Farmingdale, NY. When Fairchild aviation purchased Republic, Grumman Aircraft bought the tunnel.

7.3.2 Computational challenges/methods

The theoretical/computational transonic flow problem was very hard. Initially, very few analytic or numerical methods were available. By 1970, "everybody" was trying to come up with a method to compute the transonic flow over an airfoil (the "blunt body problem", which was important in predicting the flowfield at the nose of re-entering ballistic missiles and the manned space program,

had just been conquered, see Chapter 11). The transonic problem is difficult because it is inherently nonlinear, and the steady solution changes math types, being elliptic in the subsonic portion of the flow and hyperbolic in the supersonic part of the flow. Earll Murman and Julian Cole made the major breakthrough.[6] Using transonic small disturbance theory, they came up with a scheme that could be used to develop a practical computational method. Equation 7-1 illustrates how the nonlinear term in the equation allows for the equation to change type, and indeed provides a way for the type to be found locally in a computational scheme.

$$\underbrace{\left[1-M_\infty^2-(\gamma+1)M_\infty^2\phi_x\right]}_{\substack{>0 \text{ elliptic PDE} \\ <0 \text{ hyperbolic PDE}}}\phi_{xx}+\phi_{yy}=0 \tag{7-1}$$

In Murman and Coles's scheme shocks emerged naturally during the numerical solution of the equation. Essentially, they used finite difference approximations for the partial derivatives in the transonic small disturbance equation. The key to making the scheme work was to test the flow at each point to see if the flow was subsonic or supersonic. If it was subsonic, a central difference was used for the second derivative in the x-direction. If the flow was supersonic, they used an upwind difference to approximate this derivative. This allowed the numerical method to mimic the physical behavior of the flowfield. The nonlinear coefficient of the ϕ_{xx} term in Eq. (7-1) is a first derivative in x, ϕ_x. A central difference approximation can be used for this term. Since the solution is found by iteration, old values can be used for ϕ_x. Their approach became known as "mixed differencing," and it was a simple way to capture the physics of the mixed elliptic-hyperbolic type of the partial differential equation. Because shocks emerge during the solution process, The method is termed a "shock capturing" method, and was much simpler for a general 3D method than a competing method at the time, in which shocks were located and across which the Rankine-Hugoniot conditions were satisfied analytically. This was known as a "shock fitting" method. Although several theoretical refinements were required, their scheme led to today's codes. Hall has described the circumstances under which this breakthrough took place.[7] The code known as TSFOIL was the final development of small disturbance theory methods for 2D.[8]

After hearing Earll Murman describe his new method at the AIAA Aerospace Sciences Meeting in New York City in January of 1970, Antony Jameson, at the time working for Grumman, returned to Bethpage on Long Island, coded up the method himself, and then went on to extend the approach to solve the full potential equation in body fitted coordinates. This required several additional major contributions to the theory. The code he developed was known as FLO6,[9] and, after several more major methodology developments, resulted in the extremely efficient full potential

flow code known as FLO36.[10] These were the first truly accurate and useful transonic airfoil analysis codes. Holst has published a survey describing current full potential methods.[11]

The next logical development was to add viscous effects to the inviscid calculations, and to switch to the Euler equations for the outer inviscid flow. By now, many researchers were working on computational flow methodology, which had become an entire field known as CFD. An entrance to the literature on computational methodology is available in the survey article by Jameson.[12] The Euler solution method used here is from a code known as MSES,[13] by Prof. Mark Drela of MIT.

Figure 7-3 provides a comparison of the predictions for the transonic flow over an NACA 0012 airfoil at $M = 0.75$ and 2° angle of attack for the key inviscid flow models. In general, the results are in good agreement. However, the full potential solution predicts a shock that is too strong, and too far aft. The small disturbance theory is in close agreement with the full potential solution, while the Euler equation model, which is the most accurate of these flow models, has a weaker shock located ahead of the other methods. This occurs for two reasons. First, the potential flow model does not contain the correct shock jump. Second, there is no loss in stagnation pressure across the shock in the potential flow models, making them insensitive to the "back pressure" downstream, to use an analogy from nozzle flows.

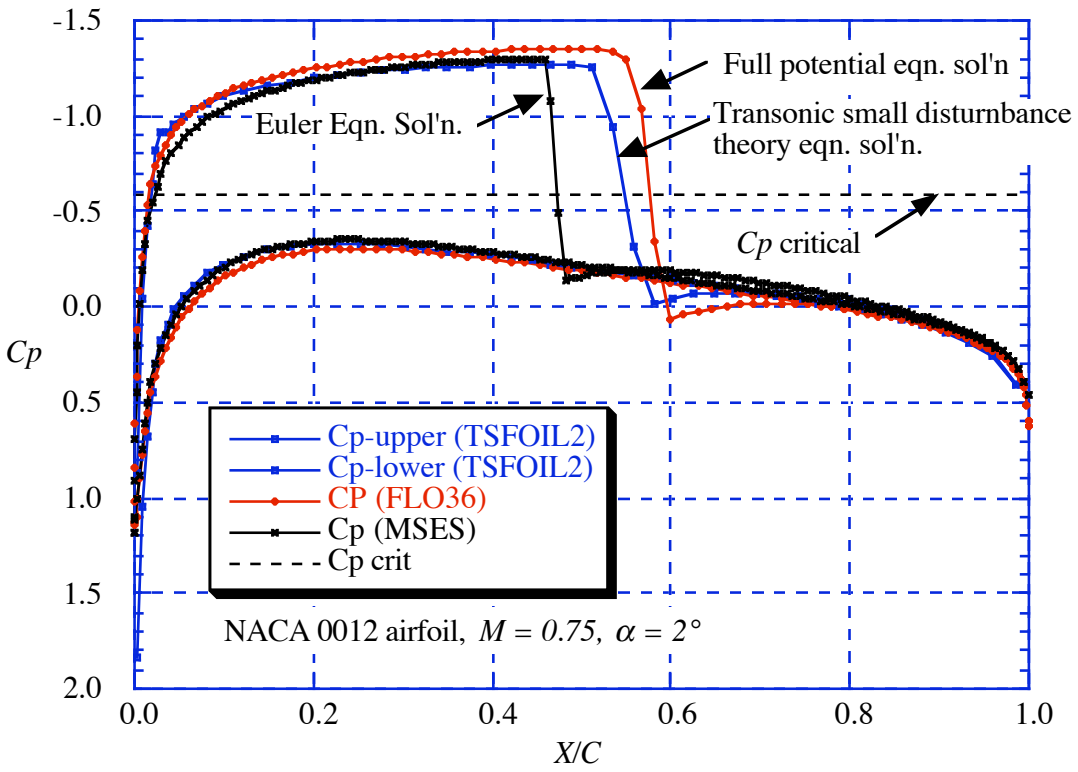

Figure 7-3. Comparison of pressure distributions on an NACA 0012 airfoil at $M = 0.75$, and $\alpha = 2°$ using three different computational methods, small disturbance theory (TSFOIL2), the full potential equation (FLO36), and the Euler equations (MSES).

Several key points need to be made while examining Figure 7-3. First, the solutions for transonic flow are found from iterative solutions of a system of nonlinear algebraic equations. This is much more difficult than the subsonic case, where the equations for panel methods are linear. The codes require much more care in their operation to obtain good results. Students often ask for solutions for flow cases that are too difficult to solve. You can't ask for a solution at $M = 0.95$ and 10° angle of attack and expect to get a result from most codes. Students should start with known cases that work, and try to progress slowly to the more difficult cases. Next, the shock is typically smeared over several grid points in the numerical solution. The actual solution point symbols have been included in the plots in Figure 7-3 to illustrate this. Finally, the region where the flow is locally supersonic can be observed by comparing the local value of the pressure coefficient to the critical value, shown on the figure as a dashed line. If the pressure coefficient at a point on the airfoil is lower (more negative) than the critical value at that point, the flow is supersonic at that point. The critical value is the point on the airfoil where, assuming isentropic flow, the value of the pressure corresponds to a local Mach number of one. The derivation of Cp_{crit} is given in any good basic compressible flow text, and the formula is:

$$C_{p_{crit}} = -\frac{2}{\gamma M_\infty^2}\left[1 - \left(\frac{2}{\gamma+1} + \frac{\gamma-1}{\gamma+1}M_\infty^2\right)^{\frac{\gamma}{\gamma-1}}\right] \tag{7-2}$$

Dedicated airfoil pressure distribution plotting packages usually include a tick mark on the Cp scale to indicate the critical value.

Next, we use the full potential equation solution to illustrate the development of the flow with increasing Mach number for the same NACA 0012 airfoil used above in Figure 7-3. Figure 7-4 shows how the pressure distribution changes from subcritical to supercritical. At $M = 0.50$, the flow expands around the leading edge and then starts to slow down. This is the typical subsonic behavior. At $M = 0.70$ the flow continues to expand after going around the leading edge, and it returns to subsonic speed through a shock wave, which is fairly weak. As the freestream Mach number increases further, the shock moves aft rapidly, becoming much stronger. In this case we are looking at inviscid solutions, and this strong shock would likely separate the boundary layer, requiring the inclusion of viscous effects to get a solution that accurately models the real flow.

The effect of changing angle of attack on the pressure distribution, using the NACA 0012, as used in Figures 7-3 and 7-4, is shown in Figure 7-5. The results are similar to the case of increasing Mach number. The solution changes rapidly with relatively small changes in angle of attack. The shock wave develops fast, with the strength increasing and the position moving aft rapidly.

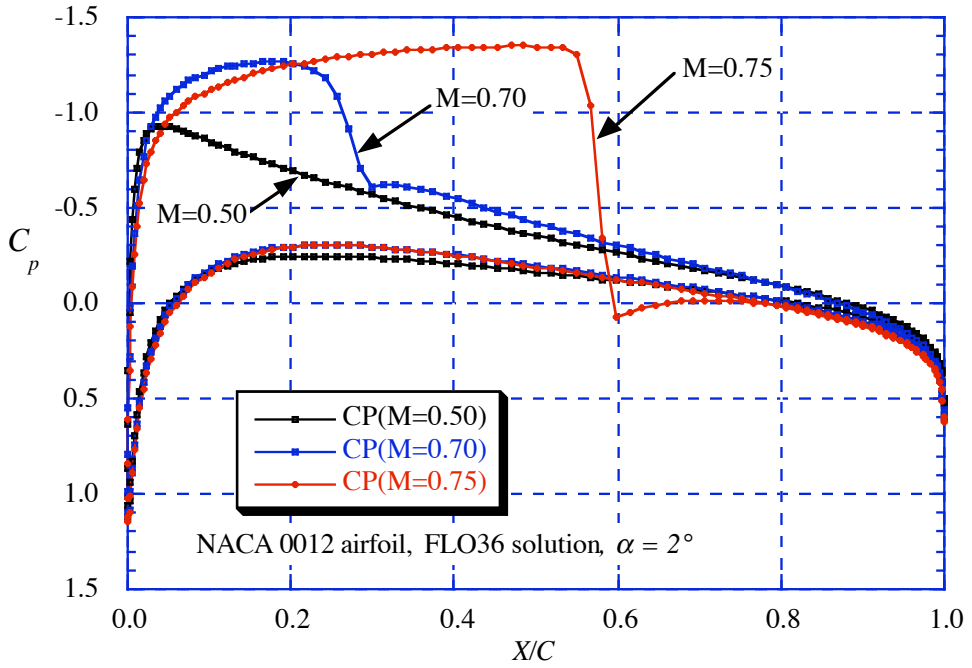

Figure 7-4. Pressure distribution change with increasing Mach number, NACA 0012 airfoil, $\alpha = 2°$.

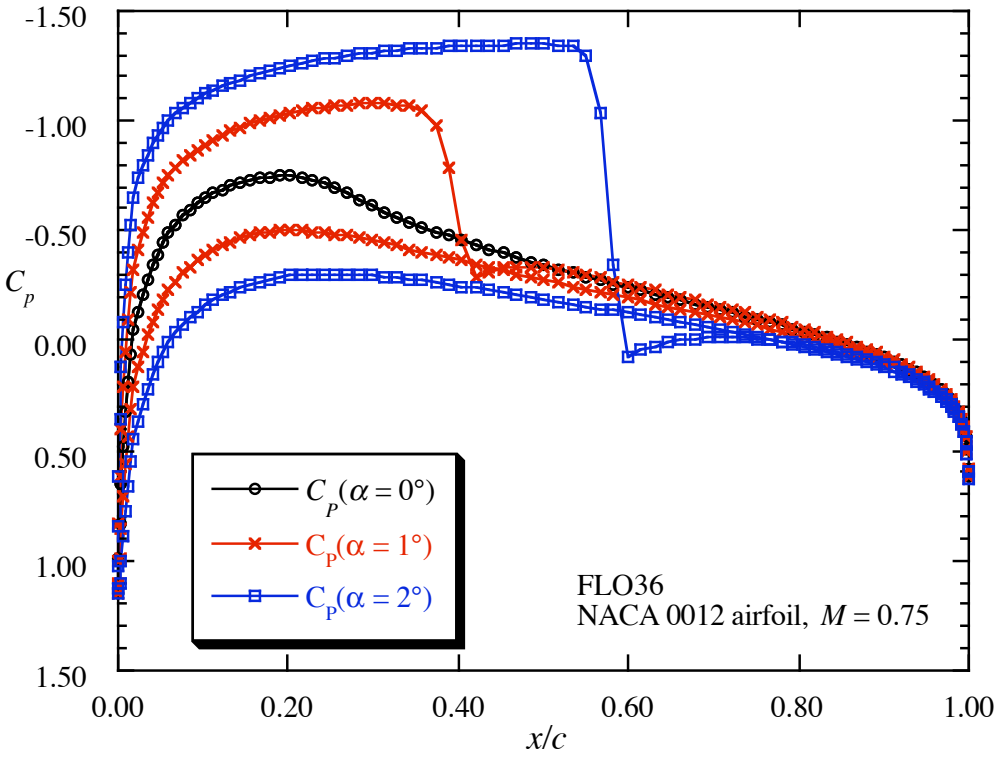

Figure 7-5. Change in pressure distribution with change in angle of attack, NACA 0012 airfoil, $M = 0.75$

7.4 Airfoils

7.4.1 *NASA Supercritical airfoils*

As described above, in the late 1960s Richard Whitcomb, at NASA Langley, developed airfoils that had significantly better transonic performance than previous airfoils. It was found that airfoils could be designed to have a drag rise Mach number much higher than previously obtained. To show how this occurs we will compare the typical transonic airfoils in use at the time, the NACA 6A series foils, with one of the NASA supercritical airfoils. Figure 7-6 contains a plot of the NACA 64A410 airfoil and its transonic pressure distribution. Figure 7-7 contains similar data for a NASA supercritical airfoil, Foil 31. The difference between these figures illustrates the modern approach to transonic airfoil design. We will discuss the differences after the figures are presented.

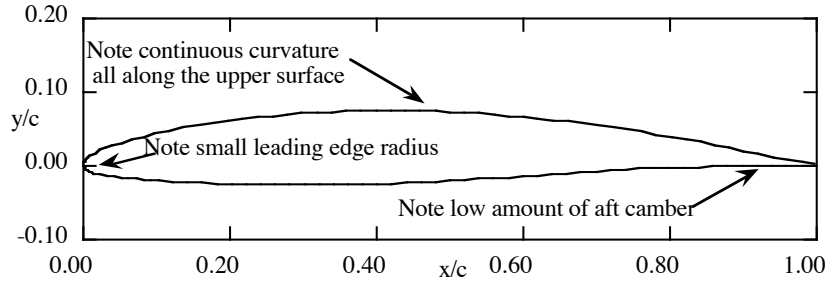

a) NACA 64A410 airfoil

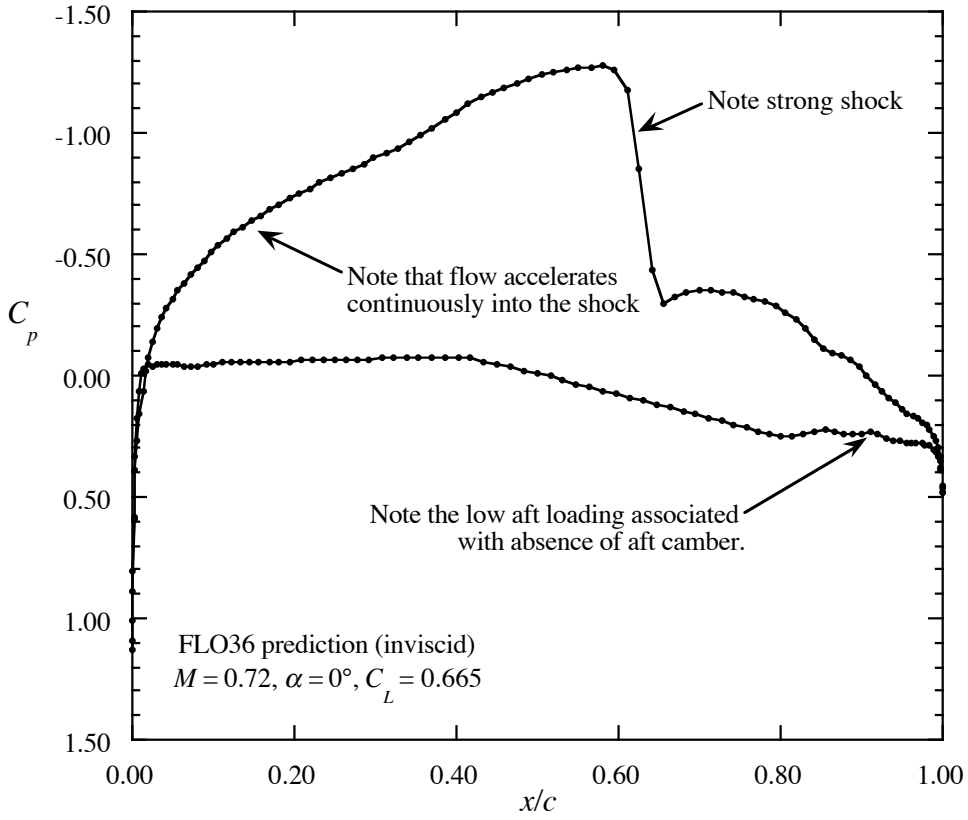

b) transonic pressure distribution on the NACA 64A410

Figure 7-6. NACA 64A 410 airfoil shape and related pressure distribution.

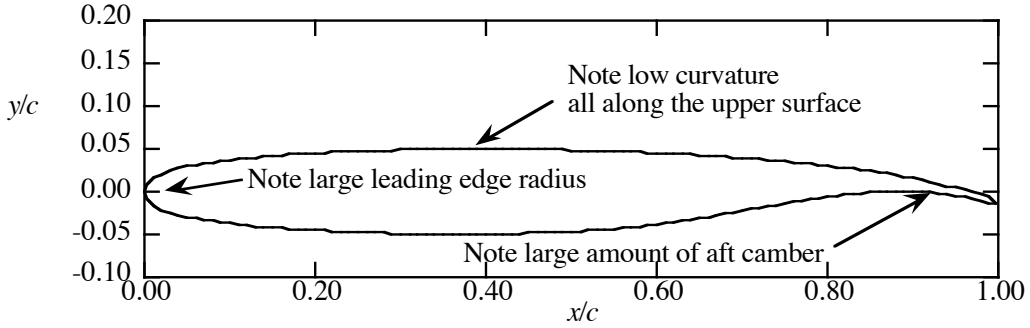

a) FOIL 31

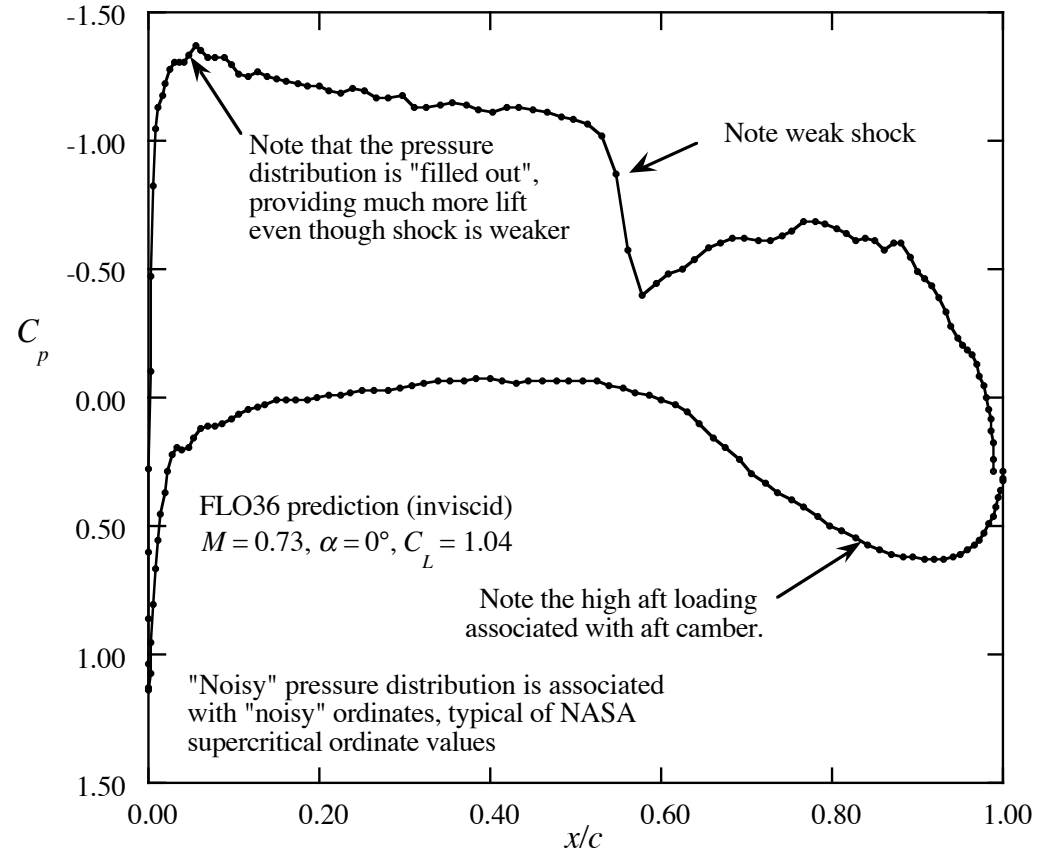

b) Transonic pressure distribution on the supercritical airfoil, Foil 31.

Figure 7-7. FOIL 31 airfoil shape and related pressure distribution.

Note that the shock wave on the supercritical airfoil is much weaker than the shock on the 64A410, even though the lift is significantly greater. This illustrates the advances made in airfoil design. Although the 6A series airfoils were widely used in transonic and supersonic applications, they were actually designed during and just after WWII to attain laminar boundary layer flow over a portion of the airfoil. They were not designed for good transonic performance (no one knew how to do this at that time). The history and development of supercritical airfoils has been described by

Harris[14], as well as by Becker, cited previously.[4] Whitcomb's original unclassified paper was presented in 1974.[15] These references should be read to get the authentic description of the development of supercritical airfoils. We will give a very brief overview here next.

Essentially, the key to transonic airfoil design to is to control the expansion of the flow to supersonic speed and its subsequent recompression. It was remarkable that Whitcomb was able to do this using an experimental approach. Because it was so difficult, he was a major proponent of developing computational methods for transonic airfoil design. Key elements of supercritical airfoils are *i*) A relatively large leading edge radius is used to expand the flow at the upper surface leading edge, thus obtaining more lift than obtained on airfoils like the 64A410, as shown in Figure 5. *ii*) To maintain the supersonic flow along a constant pressure plateau, or even have it slow down slightly approaching the shock, the upper surface is much "flatter" than previous airfoils. By slowing the flow going into the shock, a relatively weak shock, compared to the amount of lift generated, is used to bring the flow down to subsonic speed. *iii*) Another means of obtaining lift without strong shocks at transonic speed is to use aft camber. Note the amount of lift generated on the lower surface aft portion of the supercritical airfoil in Fig. 7-7b compared to the conventional airfoil in Fig. 7-6b. One potential drawback to the use of aft camber is the large zero lift pitching moment. *iv*) Finally, to avoid flow separation, the upper and lower surfaces at the trailing edge are nearly parallel, resulting in a finite thickness trailing edge. The base drag is small at transonic speeds compared to the reduction in profile drag. These are the essential ingredients in supercritical airfoil design, and modern aerodynamic designers pick the best aspect of these elements to fit their particular application.

Whitcomb cited four design guidelines for airfoil development.

1. An off-design criteria is to have a well behaved sonic plateau at a Mach number of 0.025 below the design Mach number.
2. The gradient of the aft pressure recovery should be gradual enough to avoid separation (This may mean a thick trailing edge airfoil, typically 0.7% thick on a 10/11% thick airfoil.)
3. Aft camber so that with $\alpha_{des} \cong 0$ the upper surface is not sloped aft.
4. Gradually decreasing supercritical velocity to obtain a weak shock.

Aerodynamicists in industry have also made significant contributions to transonic aerodynamic design. The best summary of transonic design for transport aircraft is by Lynch.[16] Figure 7-8 contains a summary chart developed by Lynch to identify the issues associated with leading edge radius and aft camber.

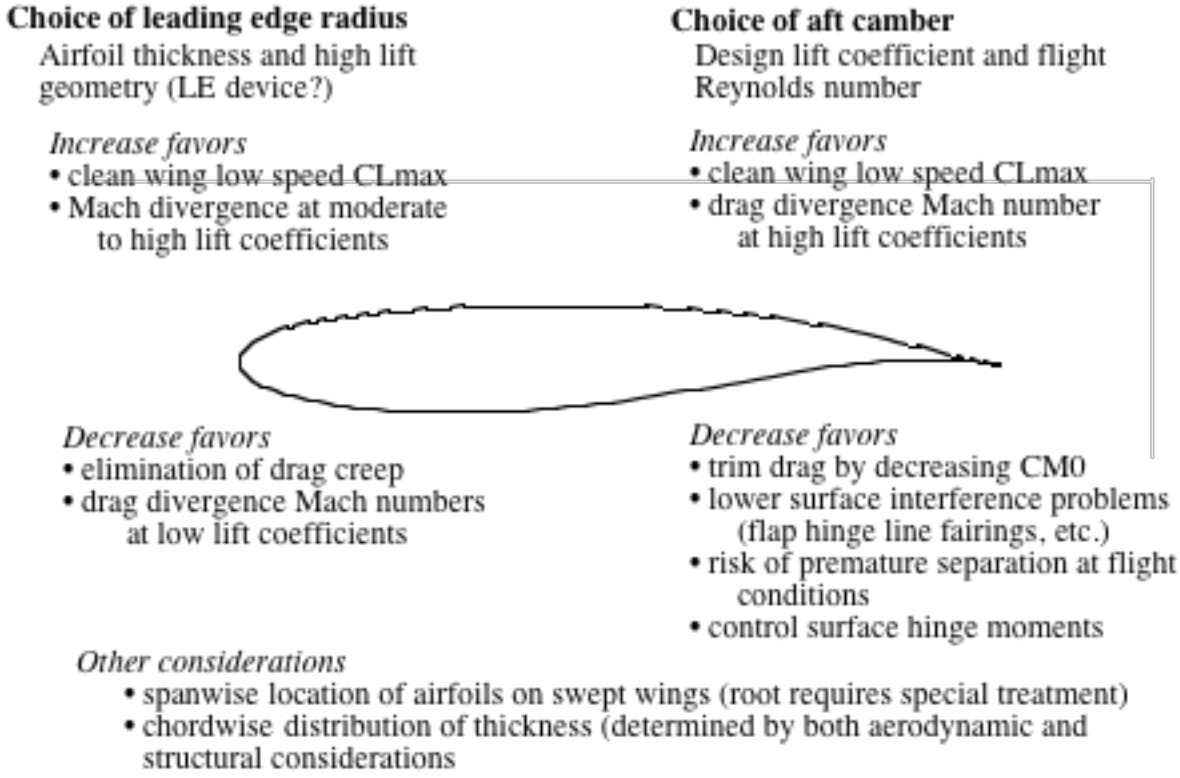

Figure 7-8. Lynch's supercritical airfoil design considerations

7.4.2 The Divergent Trailing Edge Airfoil

Just when supercritical airfoil development appeared to be completed, a further development in airfoil design was made: the divergent trailing edge airfoil. Henne and Gregg at Douglas made further improvements in airfoil performance by continuing the trend to make the upper and lower surfaces parallel at the trailing edge by using a trailing edge where the upper and lower surfaces are diverging at the trailing edge.[17] This airfoil was used on the MD-11.

7.4.3 Transonic airfoil performance: the Korn Equation

Attempts have been made to estimate the capability of transonic airfoils for the purposes of design studies without performing wind tunnel or detailed computational design work. This is important in the initial stages of aircraft design, where airfoil performance needs to be estimated before the actual airfoil design has been done. Here we provide an approximate method for estimating the transonic performance of airfoils. It is based on "the Korn equation," which was an empirical relation developed by Dave Korn at the NYU Courant Institute in the early 1970s, and in use at Grumman when I arrived in 1974. Based on his experience, it appeared that airfoils could be designed for a variety of Mach numbers, thickness to chord ratios, and design lift coefficients, but in all cases there seemed to be a limit to the combination. In particular, the Korn equation is

$$M_{DD} + \frac{C_L}{10} + \left(\frac{t}{c}\right) = \kappa_A , \tag{7-3}$$

where κ_A is an airfoil technology factor. The airfoil technology factor has a value of 0.87 for an NACA 6-series airfoil section, and a value of 0.95 for a supercritical section. M_{DD} is the drag divergence Mach number, C_L is the lift coefficient, and t/c is the airfoil thickness to chord ratio. This relation provides a simple means of estimating the possible combination of Mach, lift and thickness that can be obtained using modern airfoil design, and variations of it have been shown graphically by many authors, where the scales are often left off when presented for the public by aircraft companies. Note that the Korn equation is sensitive to the value of the technology factor.

Figure 7-9, from Mason,[18] compares the prediction from the Korn equation with other estimates. In Figure 7-9a, the estimates of both older airfoils and modern supercritical airfoil performance presented by Shevell[19] are compared, and the agreement is good, with the exception of being overly pessimistic regarding older conventional airfoils at lower thickness ratios. Figure 7-9b compares the Korn equation with NASA projections[14] for supercritical airfoils based on a wealth of data and experience. In this case the Korn equation is extremely good at lift coefficients of 0.4 and 0.7, but overly optimistic at higher lift coefficients. This type of technology representation is important in developing integrated designs. To develop each point on this type of chart represents a large effort on the part of the designer (in this case the aerodynamicist).

The extension of this method to swept wings using simple sweep theory and an approximate drag rise curve shape will be given in the section on wings, below.

7.4.4 Design Methods

We gave some general approaches and guidelines for airfoil design for transonic flow above describing Whitcomb's supercritical airfoils. Although details are "beyond the scope" (as they say) of this chapter, we should point out that there are two distinct approaches available for airfoil design. Aerodynamicists frequently use inverse methods, where a target pressure distribution is specified and the required shape (which might not exist for an arbitrary pressure distribution prescription) is found. Alternatively, optimization methods may be used, where the shape is described by a set of design variables that are then used in an optimization routine. This can be computationally expensive. In addition, many optimization methods require gradients of the solution with respect to the design variables, and modern CFD methods have been developed to obtain the sensitivity of the design to geometric and flow perturbations as part of the solution. Finally, at transonic speed we need to avoid undo sensitivity to the specified design conditions. This requires a statistical design approach. An important recent advance in this area has been made by Huyse.[20]

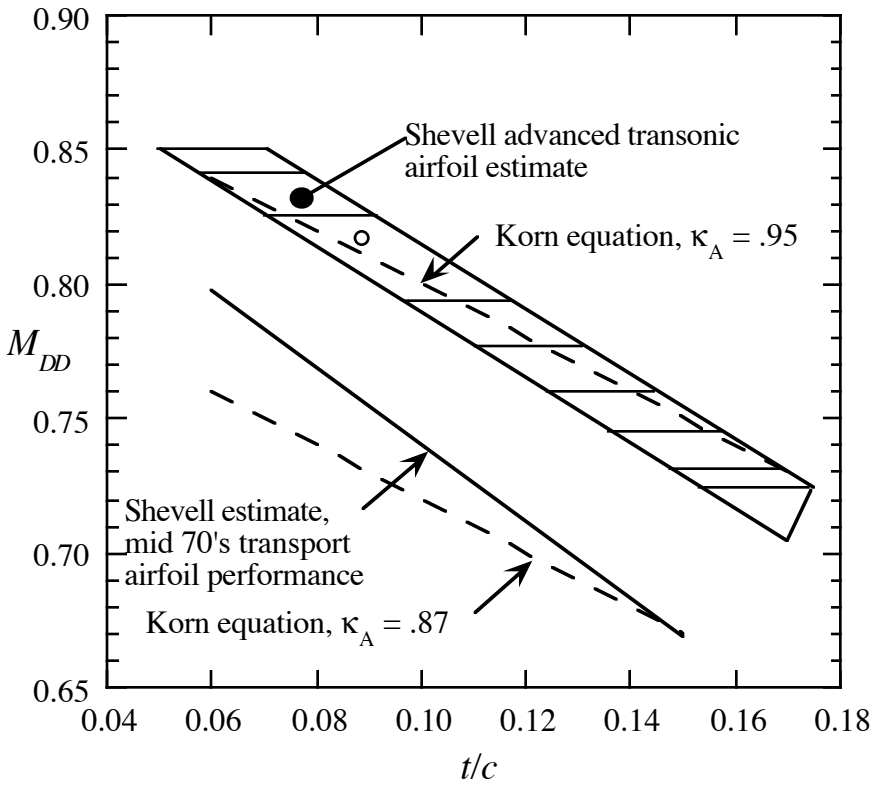

a) Comparison of the Korn equation with Shevell's estimates.[19]

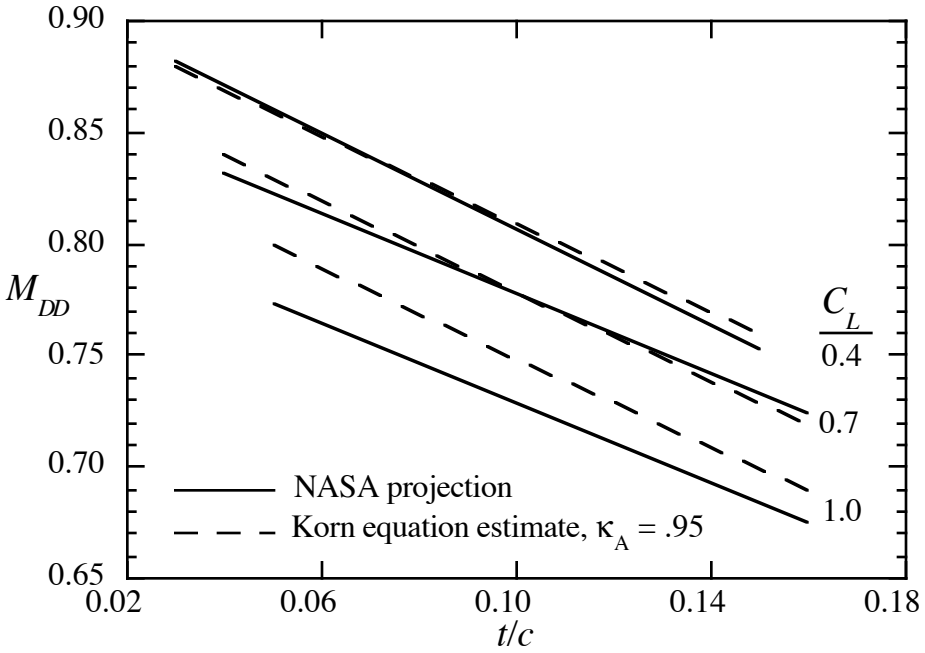

b) Comparison of the Korn equation with NASA projections[14]

Figure 7-9. Validation of the Korn equation for airfoil performance projection

7.5 Wings

We now turn our attention to wings. Today, at transonic speeds wings are swept to delay drag rise. However, even though the Boeing B-47 had a swept wing, they weren't adopted across-the-board immediately, even at Boeing. Initially, jet engines had poor fuel efficiency, and weren't considered appropriate for very long-range aircraft. In one famous instance, Boeing was working on a long-range turboprop bomber for the Air Force. When they started to present their design to the Air Force at WPAFB in Dayton, Ohio, they were immediately told to switch to a swept wing pure jet design. They didn't have time to return to Seattle, and did the work in Dayton, with the help of phone calls back to Seattle and by recruiting other Boeing engineers already in Dayton at the time. To show the Air Force the design, they made a model. Figure 7-10 shows the actual model, as displayed in the Museum of Flight in Seattle a few years ago. This design became the B-52. It is famous for having been designed in a Dayton, Ohio hotel room.

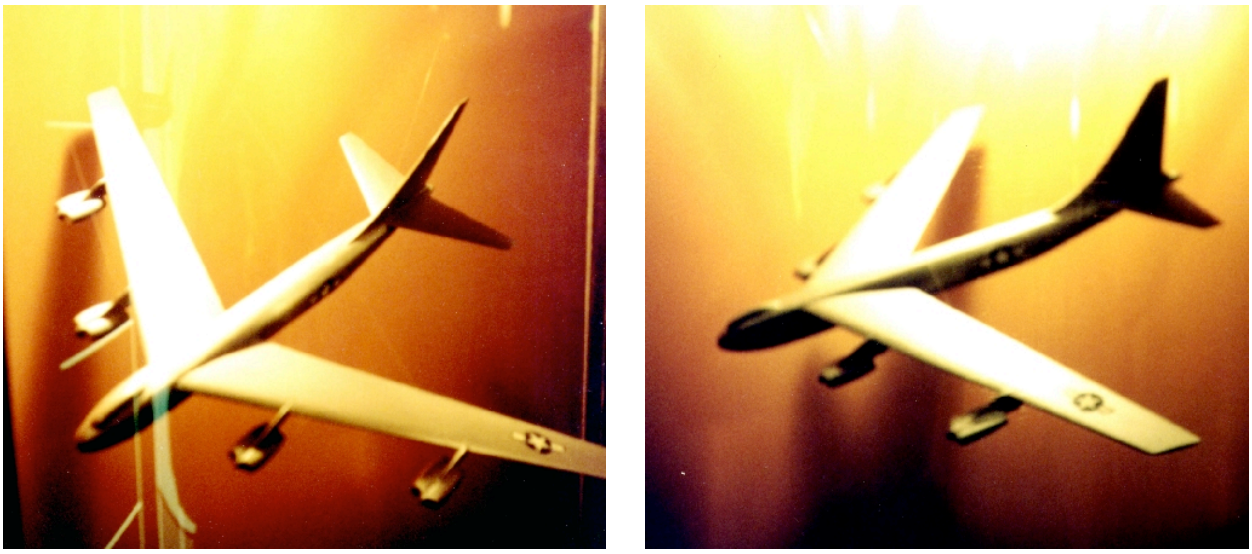

a). B-52 illustrating planform

b) B-52 illustrating high-wing mount

Figure 7-10. Model of the B-52, as carved by George Schairer, Boeing aerodynamicist, in the Van Cleve Hotel in Dayton in October 1948,[21] as displayed in the Museum of Flight in Seattle, picture by the author (note reflection because the model was displayed inside a glass case).

Although swept wings delay drag rise, there are other problems associated with swept wings, so that the aerodynamicist will want to use as little sweep as possible. Even at subsonic speed, as shown in the previous chapter, wing sweep will tend to shift the load outboard, leading to high section C_Ls, and the possibility of outboard stall, accompanied by pitchup. The wing is twisted (washed out) to unload the tip. The lift curve slope also decreases. In addition, for a given span, the actual wing length is longer, and hence heavier. High lift devices aren't as effective if the trailing edge is swept, and finally, swept wings are prone to flutter. Thus the total system design must be

considered when selecting the wing sweep. One of the benefits of advanced airfoils is that they can achieve the same performance as a wing with a less capable airfoil using less sweep. This explains the general trend to modern transports having less sweep than earlier transports.

7.5.1 Transonic Transport Wing Concepts

These wings are generally high aspect ratio swept tapered wings that clearly have an airfoil embedded in them. Generally we consider aft swept wings.

Cruise Design: Normally the aerodynamic designer is given the planform and maximum thickness and told to design the twist and camber, as well as shifting the thickness envelope slightly. He then tries to obtain "good" isobars on the wing. The natural tendency is for the flow to unsweep at the root and tip. So the designer tries to reduce this tendency to obtain an effective aerodynamic sweep as large as the geometric sweep. If possible, he would actually like to make the effective aerodynamic sweep greater than the geometric sweep. This is unlikely to happen. Generally the wing has a weak shock wave. Possibly the best tutorial paper on the problem of isobar unsweep is by Haines,[22] who is actually considering the thickness effects at zero lift.

We illustrate the problem of isobar unsweep with an example taken from work at Grumman to design the initial G-III wing (the G-III doesn't have this wing, it was considered too expensive, and the actual G-III has a highly modified version of the G-II wing). Figure 7-11 from 1978[23] illustrates the situation.

In Figure 7-11 we see the isobar pattern at transonic speed on the planform in the upper left-hand side of the figure. This wing was designed with subsonic methods, which were essentially all that was available at the time. Note that the isobars are tending to unsweep. On the upper right-hand side of the figure we see that at subsonic speed the pressure distributions at the 30% and 70% span stations lie on top of each other, the isobars are good. The lower left-hand side of the figure shows the predicted pressure distributions at these same two stations when the Mach number is increased to the transonic cruise Mach. There has been a large change in the distributions at the two stations, with the outboard shock ahead of the inboard shock. Finally, on the lower right-hand side we see the same predictions, but with wind tunnel data included. Clearly the prediction and the test results agree well and show that extra effort is required to design the wing when the flow is transonic.

Although for a given span the aerodynamicist generally prefers an elliptic spanload, it might be better for the design if the load is shifted inboard slightly, reducing the root bending moment and hence wing structural weight. [24] The optimum spanload with a winglet present is not elliptic either.

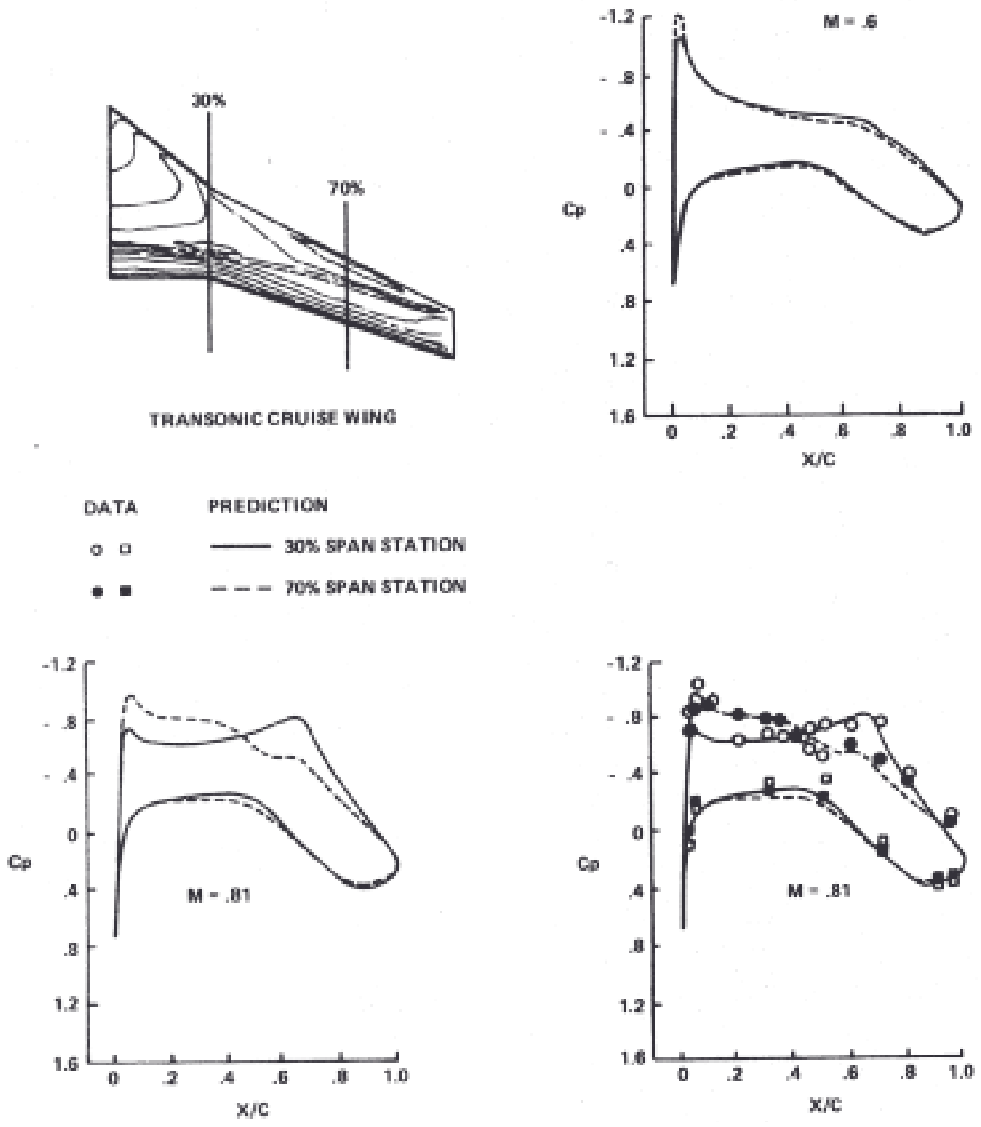

Figure 7-11. Explicit transonic three-dimensional effects.[23]

Essentially, the twist distribution is found to generate the design spanload. Note that spanloads are predicted fairly well using linear theory codes, it is primarily the chord load that reflects the nonlinearity of transonic flow. Once the basic twist is found, root and tip mods are developed to maintain the isobar pattern. Without special effort, the chord load is drawn aft at the root and shifts forward at the tip. Changes in camber and thickness are introduced to counter these effects. The planform may deviate from pure trapezoidal. In all likelihood there will be a Yehudi* at the inboard trailing edge to house the landing gear. The planform in Fig. 7-11 also has a leading edge glove inboard. This allows the t/c to be lower for the same t, and increasing the chord lowers the section c_l required to obtain the spanload required, as well as helping maintain isobar sweep. Breaks in the

* See Chapter 6 for a discussion of the so-called Yehudi flap.

planform chord distribution produce rapid variations in the section lift distribution because the spanload will tend to remain smooth. The section lift distribution may be smoothed out by using several smaller spanwise breaks. This has been done on modern Boeing and Airbus designs.

The designer also has to consider buffet margins. This means the wing C_L has to be capable of a 1.3*g* turn at the highest cruise Mach number without predicting any significant flow separation.

Other important details include nacelle/pylon interference and the resulting detailed shaping, and manufacturing constraints. This means considering the limits to curvature and the manufacturing department's desire for straight-line wrap or ruled surfaces.

Once the design starts to get close to the desired properties, local inverse methods can be applied to achieve the target pressure distributions.

Transonic Configuration Design Finally, a recent review of the design process by Jameson is worth reading to get some idea of the current design process and future possibilities.[25]

7.5.2 The Korn equation applied to drag prediction on swept wings

As described above, the Korn equation can be used to estimate the drag divergence Mach number. This equation has been extended to include sweep using simple sweep theory[18 and 26]. The result is given by:

$$M_{dd} = \frac{\kappa_A}{\cos\Lambda} - \frac{(t/c)}{\cos^2\Lambda} - \frac{c_l}{10\cos^3\Lambda} \tag{7-4}$$

This model estimates the drag divergence Mach number as a function of an airfoil technology factor (κ_A), the thickness-to-chord ratio (t/c), the lift coefficient (c_l), and the sweep angle (Λ). Recall that the airfoil technology factor has a value of 0.87 for a NACA 6-series airfoil section, and a value of 0.95 for a supercritical section.

With this approximation for the drag divergence Mach number, we can now calculate the critical Mach number. The definition of the drag divergence Mach number is taken to be:

$$\frac{\partial C_D}{\partial M} = 0.1 \tag{7-5}$$

Next, make use of Lock's proposed empirically-derived shape of the drag rise[27]

$$C_D = 20\,(M - M_{crit})^4 \tag{7-6}$$

The definition of the drag divergence Mach number is equated to the derivative of the drag rise formula given above to produce the following equation:

$$\frac{\partial C_D}{\partial M} = 0.1 = 80\,(M - M_{crit})^3 \tag{7-7}$$

We can then solve this equation for the critical Mach number:

$$M_{crit} = M_{dd} - \left(\frac{0.1}{80}\right)^{1/3} \tag{7-8}$$

where the drag divergence Mach number is given by the extended Korn equation.

Joel Grassmeyer then developed a method to compute the wave drag coefficient for use in MDO studies of a transonic strut-braced wing concept using the following relation: [28]

$$c_{d_{wave}} = 20\,(M - M_{crit})^4 \frac{S_{strip}}{S_{ref}} \qquad for\ M > M_{crit,} \tag{7-9}$$

where the local t/c, c_l, and half-chord sweep angle are specified for a number of spanwise strips along the wing, and the drag of each strip is combined to form the total wave drag. In the equation above, the wave drag for each strip is multiplied by the ratio of the strip area (S_{strip}) to the reference area (S_{ref}). The example given here uses eight spanwise strips.

This method has been validated with the Boeing 747-100, as shown in Figure 7-12. The solid lines represent the current model predictions, and the discrete data points represent the Boeing 747 flight test data. The predictions show good agreement with the data over a wide range of Mach numbers and lift coefficients. We re-emphasize that the results are sensitive to the value of the airfoil technology factor. A value of 0.89 was used for the Boeing 747 results in Figure 7-12. Based on an analysis of the Boeing 777, a value of 0.955 was used to simulate that aircraft's wave drag characteristics.

7.5.3 Fighter Wing Concepts/Issue

Bradley has given a good survey of the issues for transonic aerodynamic design of fighters.[29] We conclude this chapter with a few comments on these aspects of transonic aerodynamics.

Attached Flow Maneuver Wing Design: To push performance past the cruise lift condition the situation changes. If the goal is to obtain efficient lift at high lift coefficients using attached flow design, the emphasis switches from an elliptic loading to a span loading that pushes each section lift coefficient to its limit. Thus, if the planform is a simple trapezoidal planform with a single airfoil section, the goal is to attain a constant section C_L across the wing.[30] The penalty for a non-elliptic spanload is small compared to the additional profile drag for airfoils operating past their attached flow condition on portions of the wing. This is essentially what was done on the X-29. The so-called "Grumman K" airfoil was used on the X-29.

Two other considerations need to be addressed. Wings designed to operate over a wide range of conditions can use the leading and trailing edge devices to approximate the optimum wing shape by using a deflection schedule to automatically deflect to the best shape. Although research has been

done on smooth surfaces to do this, in most cases the devices are simply flap deflections. In the case of the X-29, the airfoil was shaped for the maneuver design point, and the devices were used to reduce the trailing edge camber at lower lift coefficients.

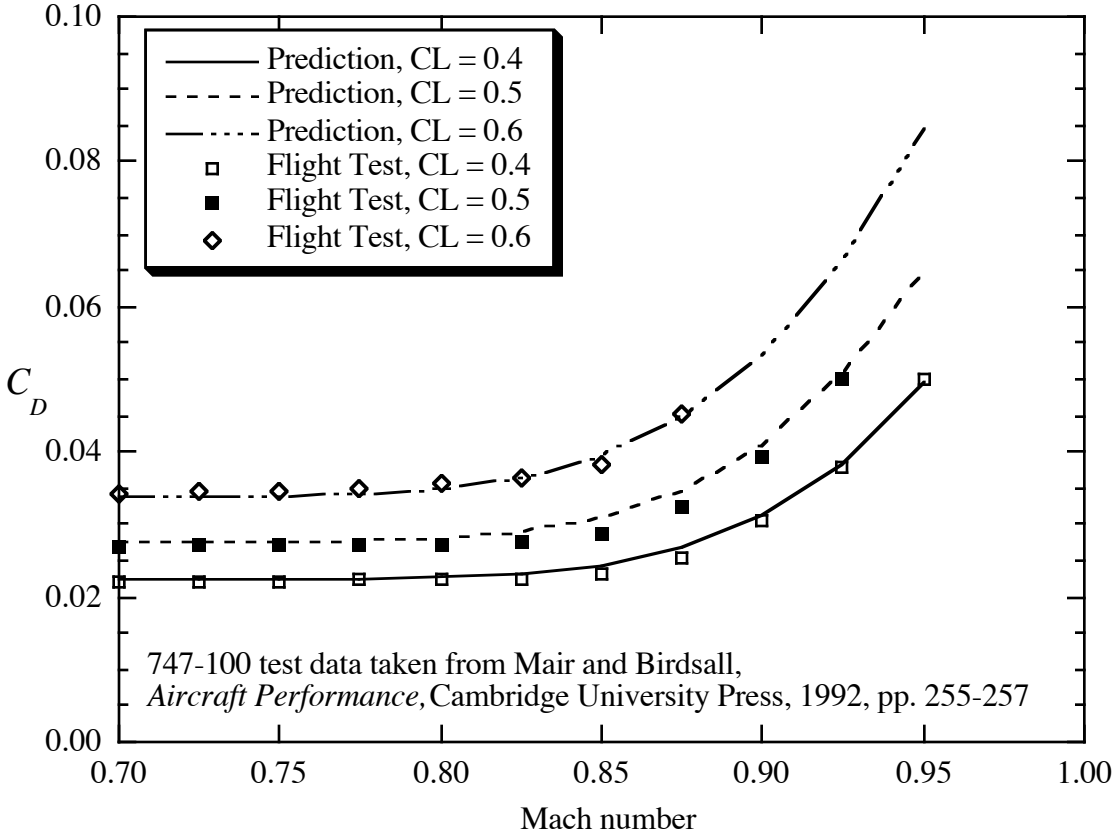

Figure 7-12: Comparison of approximate drag rise methodology with Boeing 747-100 flight test data from Mair and Birdsall[31]

The second consideration is airfoil-planform integration. If the airfoil is designed to be heavily loaded, there is likely to be a fairly strong shock well aft on the wing. To obtain low drag this shock should be highly swept. This means that the trailing edge of the wing should be highly swept. This can be done using a wing with inverse taper or a forward swept wing. This is one reason to consider a forward swept wing concept. However, a forward swept wing with a canard must be balanced with a large negative static margin to gain the full benefit of the concept. The X-29 is about 32 -35% unstable for this reason.

Finally, when the airfoils are being pushed to their limits, planform kinks are a very poor idea. The tendency of the spanload to remain smooth means that the local lift coefficients change rapidly in the kink region, and local lift coefficients often becoming excessively large.

Another alternative is to include a canard in the configuration. A canard can be used to carry additional load at extreme maneuver conditions.

Vortex Flow/Strake Maneuver Wing Design: Another method of obtaining high maneuver lift has proven effective on the F-16 and F-18 aircraft. In this case, inboard strakes are used (Northrop called theirs a LEX, leading edge extension, dating back to the F-5 days). The strakes produce a strong vortex at high angles of attack. The vortices flow over the aircraft surfaces, and as a result of the low pressure field, create additional lift. Careful shaping of the strake is required, but good performance can be obtained. Note that these airplanes also use leading and trailing edge wing device scheduling to achieve optimum performance.

Figure 7-13 shows, in a rough sense, how the two concepts compare. Here "E" is the efficiency factor in the drag due to lift term of the classic drag polar,

$$C_{D_L} = \frac{C_L^2}{\pi ARE} \tag{7-10}$$

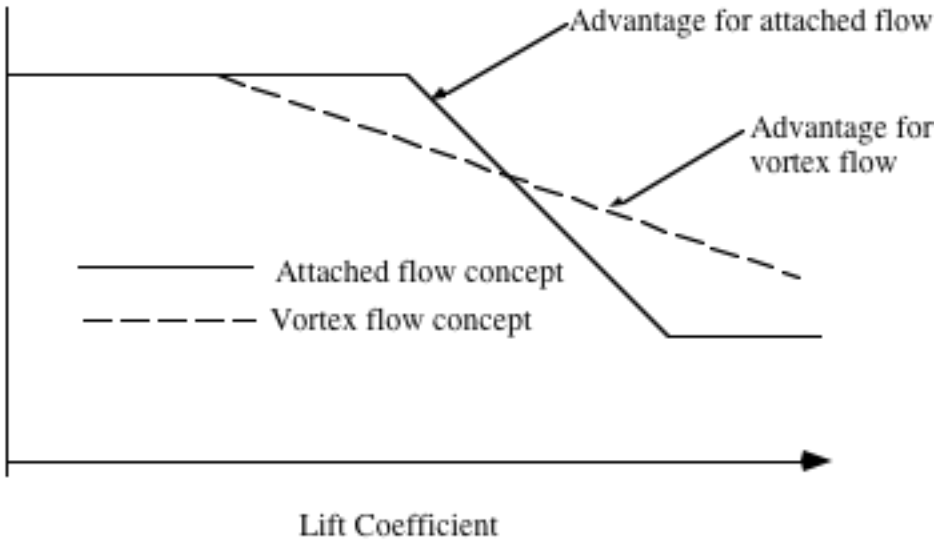

Figure 7-13. Effectiveness of various wing concepts in terms of efficiency, E.

7.6 Exercises

1. Read the paper by Frank Lynch (Ref. 16), and write a one page summary in preparation for a class discussion on the paper.

7.7 References

[1] R.L. Foss, "From Propellers to Jets in Fighter Aircraft Design," AIAA Paper 78-3005, in *Diamond Jubilee of Powered Flight, The Evolution of Aircraft Design*, Jay D. Pinson, ed., Dec. 14-15, 1978. pp. 51-64. (This paper contains the estimated drag rise characteristics of the P-38.

[2] H.H. Hurt, Jr., *Aerodynamics for Naval Aviators*, Revised edition, 1965, published by Direction of the Commander, Naval Air Systems Command, United States Navy, reprinted by Aviation Supplies and Academics, Inc., 7005 132nd Place SE, Renton, Washington 98059-3153.

[3] John V. Becker, "Transonic Wind Tunnel Development (1940-1950)," Chapter III in *The High-Speed Frontier*, NASA SP-445, 1980. A *must read* to get insight into the aerodynamic research and development process, as well as to get a physical understanding of how airfoils work and how the slotted wall tunnel evolved.

[4] John V. Becker, "Supercritical Airfoils (1957-1978)" in "The High-Speed Airfoil Program," Chapter II in *The High-Speed Frontier*, NASA SP-445, pp. 55-60.

[5] James A. Blackwell, Jr., "Experimental Testing at Transonic Speeds," in *Transonic Aerodynamics*, ed. by D. Nixon, AIAA Progress in Astronautics and Aeronautics, Vol. 81, AIAA, Washington, 1982. pp. 189-238. (Blackwell worked for Whitcomb at NASA before going to work for Lockheed)

[6] Murman, E., M., and Cole, J.D., "Calculation of Plane Steady Transonic Flows," *AIAA J.,* Vol. 9, No. 1, 1971, pp. 114-121 (presented at the 8th Aerospace Sciences Mtg., New York, Jan. 1970.)

[7] M.G. Hall, "On innovation in aerodynamics," *The Aeronautical Journal*, Dec. 1996, pp. 463-470.

[8] Murman, E.M., Bailey, F.R., and Johnson, M.L., "TSFOIL — A Computer Code for Two-Dimensional Transonic Calculations, Including Wind-Tunnel Wall Effects and Wave Drag Evaluation," NASA SP-347, March 1975. (code available on Mason's software website)

[9] Antony Jamson, "Iterative Solution of Transonic Flows Over Airfoils and Wings, Including Flows at Mach 1," *Comm. Pure. Appl. Math.,* Vol. 27, 1974. Pp. 283-309.

[10] Antony Jameson, "Acceleration of Transonic Potential Flow Calculations on Aribtrary Meshes by the Multiple Grid Method," *Proceeding of the AIAA 4th Computational Fluid Dynamics Conf.*, AIAA, New York, 1979, pp. 122-146.

[11] Terry L. Holst, "Transonic flow computations using nonlinear potential methods," *Progress in Aerospace Sciences*, Vol. 36, 2000, pp. 1-61.

[12] Antony Jameson, "Full-Potential, Euler, and Navier-Stokes Schemes," in *Applied Computational Aerodynamics*, ed by P. Henne, AIAA Progress in Astronautics and Aeronautics, Vol. 125, AIAA, Washington, 1990. pp. 39-88.

[13] Mark Drela, "Newton Solution of Coupled Viscous/Inviscid Multielement Airfoil Flows," AIAA Paper 90-1470, June 1990.

[14] Charles D. Harris, "NASA Supercritical Airfoils," NASA TP 2969, March 1990. This is the written version of a talk authored by Whitcomb and Harris given at the NASA Langley Conference "Advanced Technology Airfoil Research," March 1978. Most of the papers appeared in NASA CP 2046 (note the slight delay in publication of this paper!) The paper explains the reasoning behind the concept development and the refinement in design. A "must report", it also contains the coordinates for the entire family of airfoils and updates the research to 1990.

[15] Richard Whitcomb, "Review of NASA Supercritical Airfoils," ICAS Paper 74-10, 1974. This is the first public paper on Whitcomb's new airfoil concept.

[16] Frank Lynch, "Commercial Transports—Aerodynamic Design for Cruise Efficiency," in *Transonic Aerodynamics*, ed. by D. Nixon, AIAA Progress in Astronautics and Aeronautics, Vol. 81, AIAA, Washington, 1982. pp. 81-144.

[17] Preston Henne, "Innovation with Computational Aerodynamics: The Divergent Trailing edge Airfoil," in *Applied Computational Aerodynamics*, ed by P. Henne, AIAA Progress in Astronautics and Aeronautics, Vol. 125, AIAA, Washington, 1990. pp. 221-261. This paper takes airfoil design concepts one step further, and describes the airfoil used on the MD-11 (Although I was told this concept was used on the C-17, a close examination of the trailing edge flaps manufactured at Marion Composites, during an Aerospace Manufacturing Class tour, showed that this airfoil isn't on the plane. Email from Preston Henne confirmed this when he read an earlier version of these notes.). Rob Gregg is a co-inventor of this airfoil concept.

[18] W.H. Mason, "Analytic Models for Technology Integration in Aircraft Design," AIAA Paper 90-3262, September 1990.

[19] Richard S. Shevell, *Fundamentals of Flight*, 2nd ed., Prentice-Hall, Englewood-Cliffs, 1989, pp. 223.

[20] Luc Huyse, "Free-form Airfoil Shape Optimization Under Uncertainty Using Maximum expected Value and Second-order second-moment Strategies," NASA/CR-2001-211020, ICASE Report No. 2001-18, June 2001. http://www.icase.edu/library/reports/rdp/2001.html#2001-18

[21] Clive Irving, *Wide-Body: Triumph of the 747*, William Morrow and Co., New York, 1993, pp. 122-124.

[22] A.B. (Barry) Haines, "Wing Section Design for Swept-Back Wings at Transonic Speed," *Journal of the Royal Aeronautical Society*, Vol. 61, April 1957, pp. 238-244. This paper explains how root and tip modifications are made to make the isobars swept on a swept wing. Old, but an important paper.

[23] W.H. Mason, D.A. MacKenzie, M.A. Stern, and J.K. Johnson, "A Numerical Three Dimensional Viscous Transonic Wing-Body Analysis and Design Tool," AIAA Paper 78-101, Jan.1978.

[24] Sergio Iglesias and W. H. Mason, "Optimum Spanloads Including Wing Structural Weight," 1st AIAA Aircraft Technology, Integration, and Operations Forum, Los Angeles, CA, AIAA Paper 2001-5234, October 16-17, 2001.

[25] Antony Jameson, "Re-Engineering the Design Process through Computation," AIAA Paper 97-0641, Jan. 1997. This paper contains a good description of the transport wing design problem as currently done. Prof. Jameson does a good job of articulating the process for the non-expert wing designer, something the company experts haven't done often. This may be because they consider the process to be competition sensitive.

[26] Brett Malone and W.H. Mason, "Multidisciplinary Optimization in Aircraft Design Using Analytic Technology Models," *Journal of Aircraft*, Vol. 32, No. 2, March-April, 1995, pp. 431-438.

[27] Hilton, W.F., High Speed Aerodynamics, Longmans, Green & Co., London, 1952, pp. 47-49

[28] Grasmeyer, J.M., Naghshineh, A., Tetrault, P.-A., Grossman, B., Haftka, R.T., Kapania, R.K., Mason, W.H., Schetz, J.A., "Multidisciplinary Design Optimization of a Strut-Braced Wing Aircraft with Tip-Mounted Engines," MAD Center Report MAD 98-01-01, January 1998, which can be downloaded from http://www.aoe.vt.edu/aoe/faculty/Mason_f/MRthesis.html

[29] Richard Bradley, "Practical Aerodynamic Problems—Military Aircraft," in *Transonic Aerodynamics*, ed. by D. Nixon, AIAA Progress in Astronautics and Aeronautics, Vol. 81, AIAA, Washington, 1982. pp. 149-187.

[30] W.H. Mason, "Wing-Canard Aerodynamics at Transonic Speeds - Fundamental Considerations on Minimum Drag Spanloads," AIAA Paper 82-0097, January 1982

[31] Mair, W.A., and Birdsall, D.L., *Aircraft Performance*, Cambridge University Press, 1992, pp. 255-257.